Reflectivity Spectra for Commonly Used Reflectors

Martin Janecek

***Abstract*—Monte Carlo simulations play an important role in developing and evaluating the performance of radiation detection systems. To accurately model a reflector in an optical Monte Carlo simulation, the reflector's spectral response has to be known. We have measured the reflection coefficient for many commonly used reflectors for wavelengths from 250 nm to 800 nm. The reflectors were also screened for fluorescence and angular distribution changes with wavelength. The reflectors examined in this work include several polytetrafluoroethylene (PTFE) reflectors, Spectralon, GORE diffuse reflector, titanium dioxide paint, magnesium oxide, nitrocellulose filter paper, Tyvek paper, Lumirror, Melinex, ESR films, and aluminum foil. All PTFE films exhibited decreasing reflectivity with longer wavelengths due to transmission. To achieve reflectivity in the 380 to 500 nm range, the PTFE films have to be at least 0.5 mm thick—nitrocellulose is a good alternative if a thin diffuse reflector is needed. Several of the reflectors have sharp declines in reflectivity below a cut-off wavelength, including (420 nm), ESR film (395 nm), nitrocellulose (330 nm), Lumirror (325 nm), and Melinex (325 nm). PTFE-like reflectors were the only examined reflectors that had reflectivity above 0.90 for wavelengths below 300 nm. Lumirror, Melinex, and ESR film exhibited fluorescence. Lumirror and Melinex are excited by wavelengths between 320 and 420 nm and have their emission peaks located at 440 nm, while ESR film is excited by wavelengths below 400 nm and the emission peak is located at 430 nm. Lumirror and Melinex also exhibited changing angular distributions with wavelength.**

***Index Terms*—Fluorescence, Lambertian reflection, reflection coefficient, specular reflection.**

I. Introduction

Scintillating crystals emit light in a broad range of wavelengths, with many of them having their peak emissions located between 375 and 480 nm [1-6]. In order to convert this optical signal into a sizable electrical signal, the light has to be directed into a photodetector by the means of surrounding the scintillating crystal with a reflective material. This reflector should maximize the light collection and the reflector has to be chosen to provide high reflection coefficients at the scintillator's emission wavelengths.

Monte Carlo simulations play an important role in developing and evaluating the performance of radiation detection systems. The simulations offer a way of evaluating the system as a whole by exploring system parameters without the added cost of constructing the system or any of its components. For these simulations, the reflection's angular distribution [7] and the reflection coefficient (as a function of wavelength) has to be known for the results to be accurate.

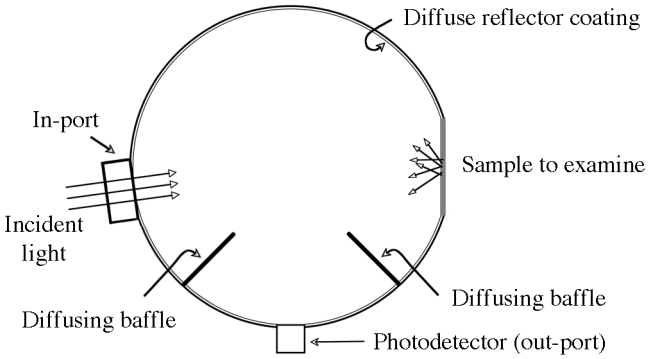

Fig. 1. Schematic of an integrating sphere. Note that the light enters at a slight angle in relation to the examined sample (~8º) in order to be able to detect the specular reflection from the sample. The inside surface of the integrating sphere is coated with a diffuse reflector creating a uniform angular distribution at the photodetector. To force the light to reflect multiple times within the integrated sphere, baffles (*i.e.*, light barriers) are located between the illuminated sample and the photodetector as well between the in-port and the photodetector, eliminating any direct optical paths.

Reflectivity measurements are generally performed with an integrating sphere, where the entire angular distribution of the reflected light is collected and thus contributes to the photodetector response. As the light is reflected many times within the integrating sphere before detection, it is important to coat the inside of the sphere with a highly reflective "white" material. The reflection data acquired using this technique do not always provide sufficient information to perform an accurate Monte Carlo simulation—some reflectors are fluorescent or change their angular reflectance distributions with incidence angle. Integrating sphere materials include barium sulfate ($BaSO_4$) [8-14], magnesium oxide (MgO) [8, 11-17], and polytetrafluorethylene (PTFE) based reflectors [18-20], and these reflector materials have been extensively studied. Other reflectors that are frequently used in optical systems include titanium dioxide (TiO_2) paint [11, 16, 21], Tyvek® paper [22, 23], ESR (Enhanced Specular Reflector) film [24, 25], and Spectralon [19, 26]. In addition, some commonly used reflectors have not been reported on in the literature, including nitrocellulose, GORE®, Lumirror®, and Melinex®.

The aim of this work is to measure the reflection coefficients as a function of wavelength for the most common reflectors used in the radiation detection field, and to screen them for fluorescence and angular distribution changes with wavelength.

Manuscript received September 23, 2011; revised December 14, 2011; accepted January 04, 2012. This work was supported by the U.S. Department of Energy under Contract No. DE-AC02-05CH11231.

The author is with the Lawrence Berkeley National Laboratory, Berkeley, CA 94720 USA (phone: 510-486-5579; fax: 510-486-4768; e-mail: mjanecek@lbl.gov).

II. Background

We previously measured the angular distribution of the reflected light at a fixed wavelength (440 nm) [7] and found ESR film and aluminum foil to be specular reflectors. The angular distributions of Spectralon, PFTE films, GORE® diffuse reflector, magnesium oxide, titanium dioxide paint, and nitrocellulose filter are best described as Lambertian (diffuse) reflectors. All Lambertian reflectors that were measured had a high (>98%) Lambertian component at low incidence angles (<50º), but a specular component appeared at high incidence angles. Lumirror®, Melinex®, and Tyvek® paper were measured to have reflection distributions that could not be described by a linear combination of specular and diffuse reflection distributions [7].

The angular reflection distribution measurements for commonly used reflectors [7] were performed at 440 nm, dictated by the use of a 440-nm solid-state laser [CrystaLaser®, Reno, NV], and we determined the reflection coefficient of the reflectors by integrating the reflected light collection over the full 2π of solid angle. However, the reflection coefficient was only determined at one single wavelength. In this work, we measure the relative reflection coefficient for commonly used reflectors over a large range of wavelengths. The results are normalized to the reflectivity of white reflection standards made out of Spectralon.

There are several confounding effects when measuring the reflection coefficient as a function of wavelength for a reflector: 1) the reflector can exhibit fluorescence, shifting some of the incident light to a longer wavelength, and 2) the angular distribution can change with wavelength, so measuring the reflectivity at a specific angle can give misleading results. Because of this, we have in this work 1) screened all reflectors for fluorescence, 2) compared the reflectors' specular and diffuse reflection behavior over wavelength, and 3) measured the reflectivity with an integrating sphere (which is insensitive to changes in the angular distribution of the reflectivity).

III. Methods

A. Reflectors

The reflectors we examined in this work are summarized in Table I. The reflectors' reflection coefficients at 440 nm were determined from literature values or manufacturer data—if available—or from our previous measurements [7]. The thicknesses of the reflectors were measured and are reported on in the table.

To achieve adequate thickness for the reflectivity measurements, several of the reflectors were measured in multiple layers, including ACE Teflon® tape, glossy PTFE tape, Tetratex® film, and Tyvek® paper. The magnesium oxide powder was painted in a 1-mm thick layer onto a black plastic holder by first dissolving the powder with ethanol. The nitrocellulose reflector was examined in the same manner as described in [7] (*i.e.*, by measuring the angular distribution over the full 2π of solid angle and integrating over the entire light distribution), however, after the original paper had already been published. The conclusions from these measurements were that the nitrocellulose reflector is an excellent reflector with >99% of the light being reflected in a Lambertian light distribution, and the reflection coefficient was determined to be 103% of the reflection coefficient for four layers of ACE Teflon® tape. The ESR film was examined for both the front and the back surfaces after all protective films and glue had been removed (with ethanol). The ESR film front-side is in this work defined as the side of the film that originally had a protective film covering it, but with no glue layer, and the backside is defined as the side that originally contained a glue layer as well as a protective film. Measurements were performed with both VM2000 and VM3000 ESR films. The Spectralon sample, which was bought from Ocean Optics as a white reflection standard for this project, is manufactured by Labsphere® and has the same model number as Labsphere's SRS-99 (Spectralon Reflection Standard) white reflection standard. The only physical difference between these two standards is their diameters—25.4 mm for the WS-1-LS versus 50.8 mm for the SRS-99.

TABLE I
Examined Reflectors

Reflector	Refl. Coeff. @ 440nm	Thickness [mm]	Source	Refl. Ref.
SRS-99 (White Standard)	0.988	10	Labsphere, Inc. North Sutton, NH	*company**
Spectralon (WS-1-LS)	0.993	10	Ocean Optics, Inc. Dunedin, FL	*company**
Teflon® tape (matte)	0.99	*n* x 0.06	ACE Hardware Oak Brook, IL	[18-20]
PTFE tape (glossy)	0.99	*n* x 0.08	*unknown origin*	[18-20]
Tetratex® film (matte)	0.99	*n* x 0.16	Tetratec™ Corp. Feasterville, PA	[18-20]
Titanium dioxide paint	0.955	0.14–0.18	Saint-Gobain Hiram, OH	*company**
Magnesium oxide	0.98	1.0	Mallinckrodt, Inc. Paris, KY	[11, 15]
GORE® diffuse reflector	0.99	0.50	W.L.Gore & Associates, Inc. Newark, DE	*company**
Nitrocellulose	1.02†	0.12	Advantec MFS, Inc. Dublin, CA	*measured*
Lumirror®	0.98	0.24	Toray, Japan	[7]
Melinex®	0.98	0.125	Dupont™ Wilmington, DE	[7]
Tyvek® paper	0.97	*n* x 0.11	Dupont™ Wilmington, DE	[7]
ESR film	0.985	0.065	3M St. Paul, MN	*company**, [25]
Aluminum foil	0.78	0.025	Kaiser Foil Northbrook, IL	[7]

** the reflection coefficient data provided by the manufacturer were used*
† the reflection coefficient was measured to be 103% of the reflection coefficient of four layers of ACE Teflon® tape at 440nm (i.e., 1.03 x 0.99) [7]

B. Fluorescence

The excitation light for our fluorescence measurements was produced by a 75W Xenon lamp [Oriel Research Arc Lamp, Oriel Instruments, Stratford, CT], which has a usable wavelength range of ~230 to 2500 nm. A narrow band of wavelengths was selected through a SP-2155 monochromator [Princeton Instruments, Trenton, NJ] before being collected at the exit-slit of the monochromator by 19 optical fibers (arranged in a vertical column). The monochromator was set to 200 μm entrance and exit slits, which is equivalent to ≤4.0 nm dispersion. The optical fibers were UV/VIS fibers with a 0.22 numeric aperture (NA). One of the optical fibers illuminated a calibrated solid-state photodetector [S2281, Hamamatsu, Japan], and this light was used to correct for the light intensity variations across the wavelength spectrum of

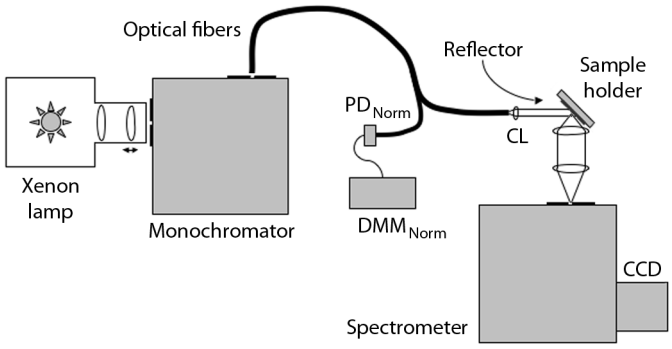

Fig. 2. Fluorescent measurement setup for reflector samples. The sample is positioned with stepper motors, and the reflected light from the sample is collected and focused into the spectrometer with two quartz lenses. The reflected light is measured over a ~500 nm wavelength spectrum with a CCD. The figure is not to scale.

the Xenon lamp and monochromator as well as any temporal variations. We used a Keithley 6517A (Keithley Instruments, Inc., Cleveland, OH) digital multimeter (DMM) to monitor the current on the solid-state photodetector. The other 18 optical fibers are bundled together and illuminated the sample, as illustrated in Fig. 2. Since the light exiting the optical fibers will diverge due to the limited numeric aperture (NA) of the optical fibers, a collimating lens was placed at the exit of the optical fiber bundle to collimate the light onto the reflector.

The reflectors were attached to a flat surface, which was covered with black tape to minimize the back surface's impact on the fluorescence measurements. The tape was analyzed in the setup and verified to be non-fluorescent. The collection beam angle (in relation to the reflector) was equal to the incidence angle. The light reflected off the sample and any fluorescent signal that was produced was collimated into a parallel beam by a 50.8-mm diameter, 50-mm focal length quartz lens, located 50 mm from the sample. The parallel light beam was then focused by a second quartz lens into a SP-2156 spectrometer [Princeton Instruments, Trenton, NJ] with a 100B charge-coupled device (CCD) [Acton Research Corporation, Acton, MA] cooled to -70ºC. The setup is illustrated in Fig. 2. The operation of the setup and all data collection was controlled by a LabVIEW program [National Instruments, Austin, TX].

We illuminated the reflector samples one wavelength at a time, stepping from 220 nm to 600 nm in 5-nm steps. At each excitation wavelength, an optical emission spectrum from 200 nm to 1000 nm was collected. Since the CCD can only record ~500 nm in a single acquisition, and since we could eliminate any second or higher order reflections from the emission spectra by using order-sorting filters, the spectrum was collected in three separate spectra: 200–360 nm (blue), 360–620 nm (green), and 620–1000 nm (red). The blue spectra were acquired with no order-sorting filters, while the green and red spectra used cut-off filters located at 320 nm and 590 nm, respectively.

C. Reflectivity measurements at fixed angles

To measure the reflectors' specular and diffuse reflectivity components as a function of wavelength, we modified the fluorescence setup described in the previous section. The illumination side of the setup was identical to the fluorescence setup, with the exception of that the monochromator was set to 50 μm entrance and exit slits. These slit widths are equivalent to ≤1.0 nm dispersion. The reflectors were attached to a flat surface, which was covered with black tape to minimize the back surface's impact on the reflectivity measurements. For the specular samples (*i.e.*, the ESR films, Aluminum foil, and Tyvek® paper), the reflector sample was placed in relation to the incident light beam so the incidence angle (the angle between the optical fibers' direction to the normal of the reflector) was equal to the reflection angle (the angle between the normal of the reflector to the centerline of the collection lens), making sure that all specular light was directed onto the center of a second S2281 photodiode. This photodiode was read out by a Keithley 485 DMM (Keithley Instruments, Inc., Cleveland, OH). For the diffuse samples, measurements were performed both with the reflection angle equal to the incidence angle (*i.e.*, a specular setup), and a setup where no specular light was allowed to make it onto the photodiode (*i.e.*, a diffuse setup). In practice, the sample was placed at 45º and 60º (relative to the incident beam) for the specular and diffuse setups, respectively, with the incident light beam and the photodetector being placed 90º apart. For the specular measurements, the photodetector was placed at a distance that created a cone with a 6.0º half-angle for the photodetector, which is equivalent to <0.5% of the 2π solid angle, and for the diffuse measurements the distance between the sample and the photodetector was decreased, which led to a 19º photodetection half-angle, which is equivalent to a 5.5% solid angle coverage.

The readout of the DMMs and the movement of the monochromator were controlled by a LabVIEW program, and the acquired data was saved to a text-file for post-processing. Each current measurement was calculated as an average of 10 individual current measurements, and the value was only accepted if the standard deviation within the ten samples was below 1% of the average value. If the standard deviation of the current was above 1%, indicating transient currents and not a steady-state current, the current was re-measured until the condition was met.

We illuminated the reflector samples one wavelength at a time, stepping from 230 nm to 800 nm in 2-nm steps. No order-sorting filters (to remove higher order light) were used. We estimate the absence of order-sorting filters to produce an error for our results of <1%.

The measured reflected light intensity was normalized at each wavelength against a white standard (SRS-99), *i.e.*, a sample that has a well-defined reflection coefficient at certain wavelengths, enabling us to translate our relative reflectivity values to absolute values across the wavelength spectrum. Since the reflection coefficient for the white standard is defined from 250 nm to 2500 nm, we only report on our measured reflection coefficients down to 250 nm. We had access to two white standards, and we compare the results obtained from both these standards. Both white standards are made out of Spectralon, a polytetraflouroethylene (PTFE) based Lambertian reflector [19, 26]. Each reflection spectrum measurement was performed at least five times (with different illumination spots on the sample) to evaluate consistency.

Since these measurements do not collect all the light (i.e., the full 2π of solid angle), the reflection coefficient curves were normalized to literature values at 440 nm. If the

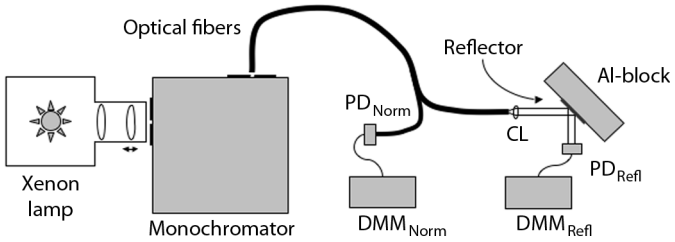

Fig. 3. Modified reflectivity measurement setup. The Xenon lamp's light is focused with two lenses into a monochromator, where a narrow band of wavelengths is selected. Most of the light is then guided to the reflector, where a collimating lens (CL) focuses the light onto the reflector sample, and a smaller portion of the light is monitored in a single strand of the optical fibers with a photodiode for normalization purposes (PD_{Norm}). The sample is attached to an Aluminum block, and the reflected light is measured in a second photodiode (PD_{Refl}). The photodiode currents are measured with digital multimeters (DMMs). The figure is not to scale.

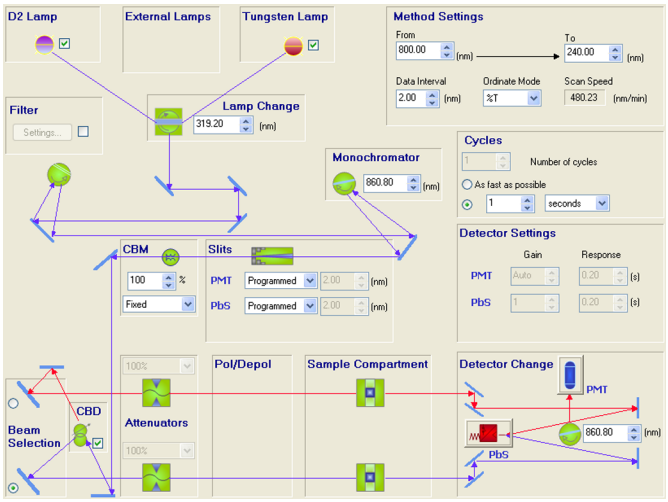

Fig. 4. Control panel (screen shot) for the reflectivity measurements performed with the Lambda 950 UV/VIS spectrophotometer and an integrating sphere. See article text for details.

normalized specular and the diffuse measurement curves were equal, we assumed that the angular distribution does not change with wavelength.

D. *Reflectivity with an Integrating Sphere*

We also measured all the reflector samples in a Lambda 950 UV/VIS spectrophotometer [PerkinElmer, Inc., Waltham, MA]. The screen shot of the control panel illustrating the setup is shown in Fig. 4. A deuterium lamp is used for the shorter wavelengths (<319nm) and a Tungsten lamp is used for the longer wavelengths when illuminating the reflector sample. The entrance and exit slits on the monochromator were set to produce 1.0 nm dispersion. The sample is placed at ~8º incidence angle, and all the reflected light is collected by the integrating sphere to a photomultiplier tube. A second beam, created from the incidence beam with a beam splitter, is used to correct for temporal intensity fluctuations in the measurements. The reflection coefficient was measured every 2 nm. The measurements were normalized to the white standard (SRS-99). Each measurement was performed three times to evaluate consistency.

IV. Results

A. *Fluorescence*

The only reflectors listed in Table I that exhibited fluorescence were the ESR films, Lumirror®, and Melinex®. All of these three reflectors exhibited strong fluorescence and their fluorescence spectra are shown in intensity plots in Fig. 5. Fig. 5(a) shows the fluorescence plot for the ESR film, Fig. 5(b) shows fluorescence for the glue that was originally attached to the backside of the ESR film, and Fig. 5(c) shows the fluorescence for Melinex®, respectively. All the ESR films exhibited very similar fluorescence, and the only noticeable difference in all the ESR film measurements was that the VM3000 film had a slightly stronger fluorescent signal for excitations below 280 nm compared to the VM2000 film. There was virtually no difference between the front- and backsides of each ESR film. The Lumirror® and Melinex® fluorescence were virtually identical, and only the Melinex® fluorescence plot is therefore displayed.

A fluorescence signal was detected from both sides (and for both versions) of the ESR film. The emission peak for the ESR film's fluorescent signal is located at 430 nm, and is produced by wavelengths shorter than 400 nm. The glue that was removed from the backside of the ESR films was measured separately for fluorescence on a (non-fluorescent) black tape. The glue's fluorescent signal has its emission peak located at 290 nm, and the glue is excited by wavelengths between 250 and 285 nm. Lumirror® and Melinex® have their emission peaks located at 440 nm, and are excited by wavelengths between 320 and 420 nm. Profiles through the emission (and excitation) maxima are shown in Figs. 6 and 7; Fig. 6 shows the profiles for the ESR film and the ESR glue, and Fig. 7 shows the profiles for Lumirror® and Melinex®.

B. *Specular reflectors*

The reflection coefficients as a function of wavelength are displayed in Fig. 8 for the specular reflectors, *i.e.*, the ESR films and the Aluminum foil, as well as for the Tyvek® paper. The protective films from the ESR films and the glue layer from the ESR backsides were removed (using ethanol) prior to any reflection (or fluorescence) measurements. As can be seen in Fig. 8, the VM3000 front-side and the VM2000 backside are virtually identical. In the same way, the VM3000 backside and the VM2000 front-side are virtually identical above 380 nm – below 380 nm the VM2000 front-side has a lower reflection coefficient. The difference between the front- and backsides for both films above 380 nm is minimal, though we did measure a 5 to 6 nm difference in the cut-off reflection wavelength between the two sides (at ~395 nm).

Tyvek® paper displays high reflection coefficients for all measured wavelengths, staying above 95% for wavelengths above 355 nm, and above 90% for wavelengths above 300 nm. Aluminum foil displays a flat reflectivity curve, with reflection coefficients between 70% and 80% above 265 nm.

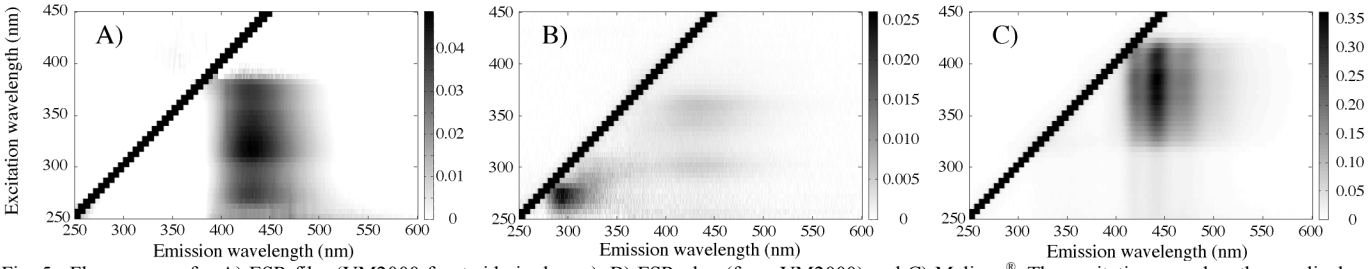

Fig. 5. Fluorescence for A) ESR film (VM2000 front-side is shown), B) ESR glue (from VM2000) and C) Melinex®. The excitation wavelengths are displayed on the vertical axis, and the resulting intensity in the emission is shown along the horizontal axis. A reflection line is clearly visible in all plots, where the excitation and emission wavelengths are equal. The highest intensity in each plot (excluding the reflection line) has been used to normalize the intensity scales.

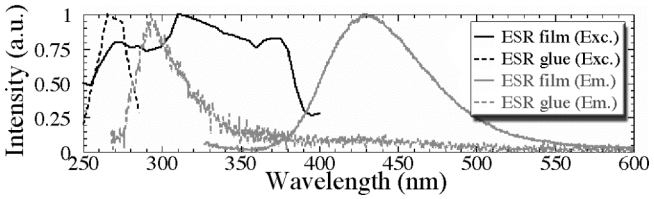

Fig. 6. Excitation and emission profiles for ESR film and ESR glue. The profiles are taken from data from Figs. 5(a) and 5(b) and pass through the maximum value in the fluorescence spectra.

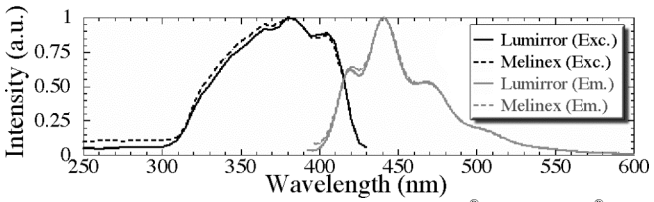

Fig. 7. Excitation and emission profiles for Lumirror® and Melinex®. The profiles are taken from data from Fig. 5(c) and the Lumirror® data (not shown) and pass through the maximum value in the fluorescence spectra.

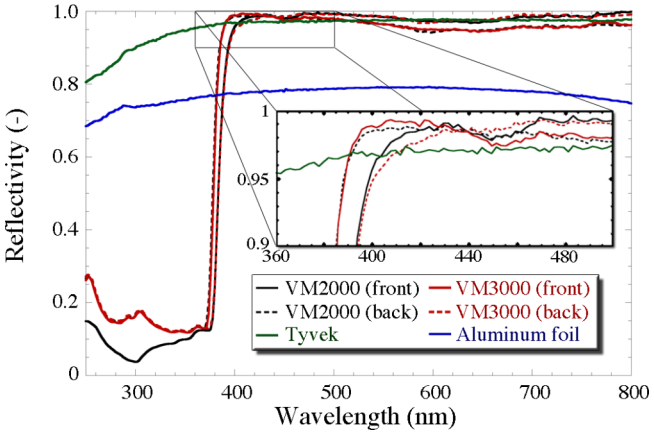

Fig. 8. Reflection coefficient for the front- and backsides of two versions of ESR film, Tyvek® paper, and Aluminum foil as a function of wavelength. The insert shows a zoom-in of the reflection data between 360 and 500 nm. The data were acquired in the specular setup of the *Reflectivity measurements at fixed angles* setup and normalized to the reflectivity values in *Table I*. The maximum error was measured to be <2%, and the average error for all the data points presented above was measured to be <0.7%.

C. *Diffuse Reflectors*

The reflection coefficients as a function of wavelength for Spectralon (WS-1-LS), GORE® diffuse reflector, MgO powder, TiO_2 paint, and nitrocellulose filter paper are displayed in Fig. 9. A zoom-in image of the wavelength range from 360 to 500 nm is also shown in the figure. The

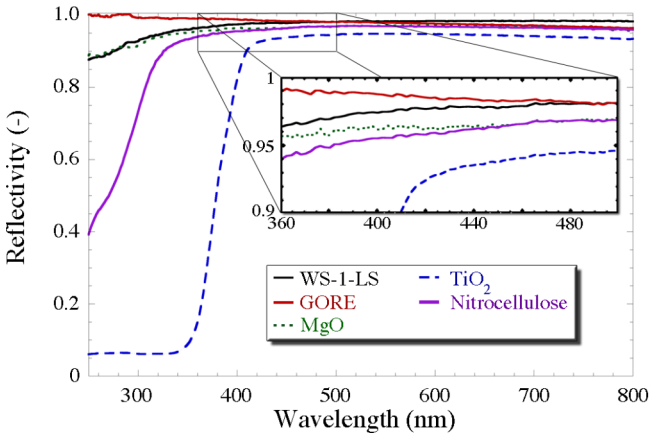

Fig. 9. Reflection coefficient for several diffuse reflectors as a function of wavelength. The insert shows a zoom-in of the reflection between 360 and 500 nm. The data were acquired in the *Reflectivity with an Integrating Sphere* setup. The measurements have *not* been normalized to the reflectivity values in *Table I* since the Lambda 950 instrument is calibrated.

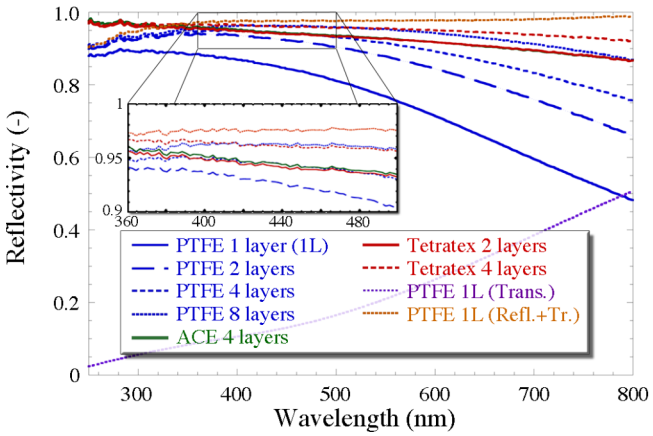

Fig. 10. Reflection coefficient for PTFE tapes as a function of wavelength. The insert shows a zoom-in of the reflection between 360 and 500 nm. The data were acquired in the *Reflectivity with an Integrating Sphere* setup. The measurements have *not* been normalized to the reflectivity values in *Table I* since the Lambda 950 instrument is calibrated.

GORE® diffuse reflector exhibits an excellent reflectivity (>98%) for wavelengths between 250 and 500 nm, while MgO and Spectralon—two materials commonly used as white reflectors—drop below 90% reflectivity for wavelengths shorter than 280 nm. Nitrocellulose and TiO_2 paint exhibit sharp declines in their reflectivity for wavelengths below 330 and 420 nm, respectively.

The reflection coefficients as a function of wavelength for PTFE tapes (glossy PTFE tape, ACE Teflon® tape, and

Tetratex® film) are displayed in Fig. 10. As described in detail in the following paragraph, all films have a decreasing reflectivity with increasing wavelength due to transmission. The transmission for a single layer of glossy PTFE film is also presented in the figure, as well as the sum of the reflected and transmitted signal, *i.e.*, 1 – absorbed. The transmission was measured by placing the reflector in the incident beam's path into the integrating sphere.

The PTFE reflectors are bulk reflectors (as opposed to surface reflectors) and longer wavelengths penetrate deeper into (or though the material). For instance, a single layer of the 80 µm thick glossy PTFE tape allows a significant amount of light (>10%) transmitted for wavelengths longer than 380 nm. By increasing the number of layers, the reflectivity increases, and at for instance 440 nm, goes from a reflection coefficient of 85% (1 layer) to 92.6% (2 layers), to 94.4% (4 layers), and to 96.2% (8 layers). In order to achieve at least 95% reflectivity for scintillator light emissions (*i.e.*, 380–500 nm), the examined PTFE films will need to be at least 0.5 mm thick. A good alternative, if a thin diffuse reflector is needed, is to use nitrocellulose.

D. *Changing angular distributions*

The Lumirror® and Melinex® reflection coefficients as a function of wavelength were measured to be different in the specular and diffuse reflection measurements. Because of this, we decided to measure the reflection over a larger range of reflection angles. The results from these measurements are displayed in Fig. 11 for Lumirror®. Melinex® exhibited similar behavior. The results in Fig. 11 have not been normalized to the reflection coefficient at 440 nm and hence show the intensity variations with reflection angle. Since the incident beam and the photodetector are place 90º apart, the 45º-setup is a specular measurement, while all the other angle-setups measure various components of the diffuse spectra. As can be seen, the slope above 400 nm, as well as the intensity of the reflection peak at 260 nm (in relation to the baseline of the reflection spectrum) varies with reflection angle. Since these two reflectors are fluorescent, a measurement in the integrating sphere produces artificially high reflection coefficients in the 320 to 420 nm wavelength range, where the quantum efficiency for the photomultiplier tube is higher for the fluorescent light compared to incident light, see Fig. 12. Lumirror® and Melinex® have a decreased reflectivity below a cut-off wavelength of 325 nm.

E. *White standards*

The manufacturers' reflection coefficient data for the two white standards are displayed in Fig. 13. The measured reflection coefficients for the WS-1-LS standard, when normalized to the SRS-99 standard, are also displayed in the figure.

V. Discussion

The high reflectance value of nitrocellulose presented in Table I indicates that the reflectivity of the ACE Teflon® tape sample—the reflector the nitrocellulose sample was normalized against—is lower than reported values [18-20]. We do not believe that this is due to improper care of the

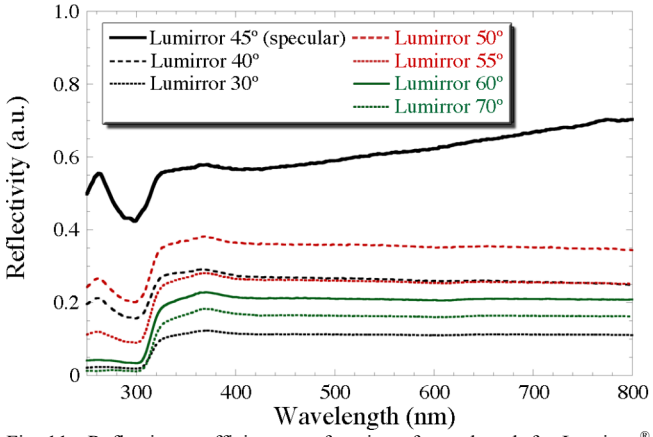

Fig. 11. Reflection coefficient as a function of wavelength for Lumirror® for a variety of reflection angles. The 45º-setup measured the specular component of the reflectivity spectra, while the other angle-setups measure various components of the diffuse spectra. The data were acquired in the *Reflectivity measurements at fixed angles* setup. The measurements have *not* been normalized to the reflectivity values in *Table I*.

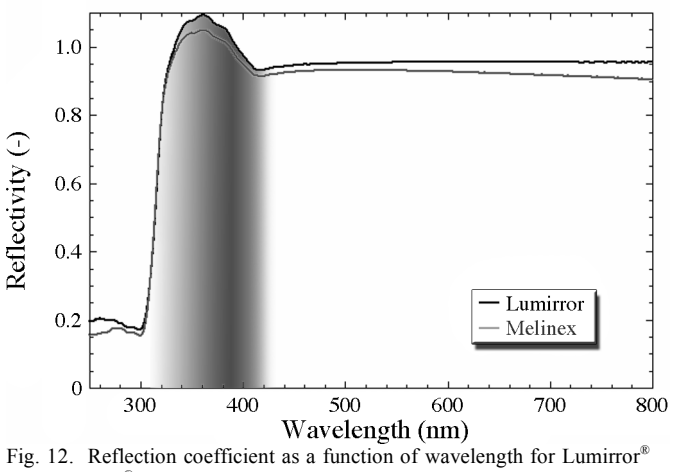

Fig. 12. Reflection coefficient as a function of wavelength for Lumirror® and Melinex®. The data were acquired in the *Reflectivity with an Integrating Sphere* setup, and the fluorescence contribution to the signal between 320 and 420 nm (shown in grey shading) produces an artificially high signal since the quantum efficiency for the photomultiplier tube is higher for the emitted wavelength than for the incident wavelength. The measurements have *not* been normalized to the reflectivity values in *Table I*.

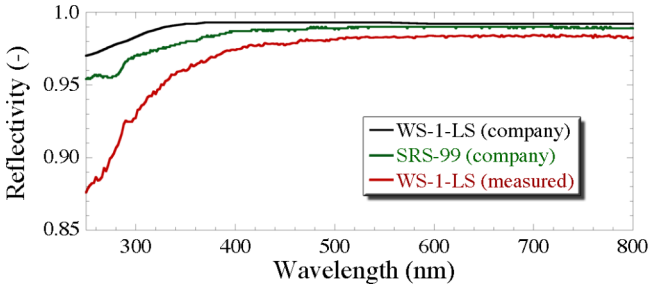

Fig. 13. Reflection coefficient as a function of wavelength for the two white standars, WS-1-LS and SRS-99 (both Spectralon). Note that the "Reflectivity"-axis scale is from 0.85 to 1.0 (and not 0 to 1) in order to enhance the differences between the curves. The data for the SRS-99 were supplied by the manufacturer. The data for the WS-1-LS were supplied by the manufacturer and acquired in the *Reflectivity with an Integrating Sphere* setup. The measurements have *not* been normalized to the reflectivity values in *Table I*, since the Lambda 950 instrument is calibrated.

samples (they were stored at stable temperatures and out of sunlight, the surfaces were clean, contact with chemicals and exposure to UV light was avoided, etc.) but attribute it instead to transmission of light through even thick layers of PTFE tape. The measurements presented in Fig. 10 show that there is a very large amount of transmission through PTFE films, and that the values reported in the literature must assume very thick or dense samples. The reflection coefficients at 440 nm were in this work measured to be 0.944 for ACE Teflon® tape and 0.962 for nitrocellulose, respectively, which gives nitrocellulose a 1.9% higher reflection coefficient at 440 nm than four layers of ACE Teflon® tape.

The intensity scales shown on the right of each fluorescence plot in Fig. 5 should not be used as absolute scales, as the size of the reflectors and the reflectors positioning in relation to the incident beam and the light collection lens play a very significant role in the detected light intensity. Although the fluorescence setup can be used to measure the reflection coefficient by filtering out any unwanted fluorescence and higher order signals, the alignment of the collimated light from the optical fibers, the sample, and the "sweet spot" from which the light collection lenses focus the light into the spectrometer (see Fig. 2), is a very delicate operation and small variations in the positions of any of these three parameters easily lead to inconsistent (*i.e.*, inaccurate) results in intensity. For this reason, although this setup is able to detect and characterize fluorescence emission and excitation wavelengths, it should not be used for absolute intensity measurements. For instance, Lumirror® and Melinex® exhibit nearly identical fluorescence spectra, and Lumirror® is only slightly brighter compared to Melinex® under a black light (excited at 365 nm), yet the measured intensity in Fig. 5C for Melinex® exhibited a four times weaker signal than for the Lumirror® fluorescence data (not shown).

Fluorescent light is isotropic in its nature, and the directionality of the light will therefore be lost for the light that interacts with the fluorescent reflector and is reemitted. Therefore, the fluorescence exhibited by the ESR films, Lumirror®, and Melinex® can be beneficial if the directionality of the light is not an issue and if the photodetector has higher quantum efficiencies at the emission wavelengths compared to the incident wavelengths. This effect is clearly demonstrated for the Lumirror® and Melinex® reflectors, as shown in Fig. 12.

The temporal behavior of the fluorescent emissions was measured in an IBH FluoroHub [HORIBA Jobin Yvon Inc, Edison, NJ] by exposing the reflectors to pulsed LED light close to the reflectors' maximum excitation wavelengths. The pulsed LEDs we had access to have emission peaks located at 268 nm (used for the ESR glue), 311 nm (ESR film), and 370 nm (Lumirror® and Melinex®). The fluorescent light emission as a function of time was measured for each reflector through a monochromator in which the signal was filtered into a narrow bandwidth (1 nm) centered at the emission peak at 430 nm (ESR film) or 440 nm (Lumirror® and Melinex®). The ESR glue was measured at 300 nm (instead of 290 nm) to minimize the light contributions from the LED's emissions. Each measurement was performed until we accumulated 10,000 counts in the peak bin. The count rate for the ESR glue signal was several orders of magnitude smaller (10^3) due to lower efficiencies of the light and the photodetector and due to the lower fluorescence, and only 5,000 counts were acquired for this material. Since the background signal is proportional to the acquisition time, the ESR glue also exhibited a much lower signal-to-noise ratio (by $>10^2$). The temporal emission curves are displayed in Fig. 14. The ESR film's fluorescence was measured to have a half-life of 14 ns, the ESR glue's fluorescence was measured to have a half-life of 7 ns, while the Lumirror® and Melinex® fluorescent half-lives were measured to be ~1 ns.

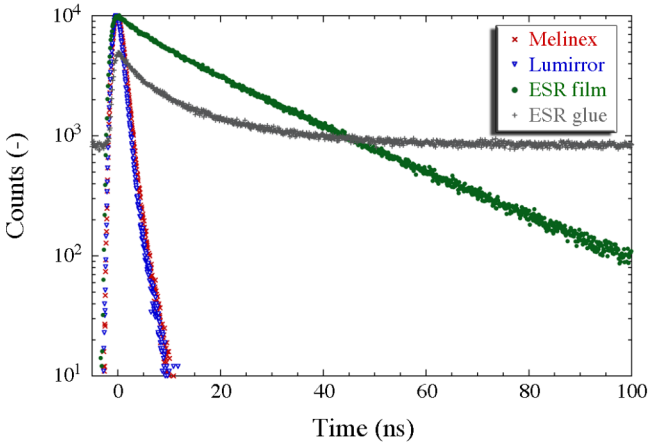

Fig. 14. Temporal behavior of the fluorescent light emitted from the reflectors that exhibited fluorescence. Note that the vertical scale is logarithmic.

Several reflectors exhibited "cut-offs" for the reflectivity for shorter wavelengths, including TiO_2 (420 nm), ESR film (395 nm), nitrocellulose (330 nm), Lumirror® (325 nm) and Melinex® (325 nm). The lower reflection coefficients below the cut-off wavelengths have to be taken into consideration when pairing up a scintillator with a reflector, by taking into account the scintillator's emission spectrum and the reflector's reflection coefficients at these wavelengths.

Our measurements showed great repeatability, where the reflection coefficient between several runs in the Lambda 950 UV/VIS spectrophotometer were typically within 0.1% of each other, and never more than 1%, and the accuracy in our measurements are thus closely tied to the accuracy of the reference standard. The data in Fig. 13 indicate that the white reflection standards often used for these measurements can be a source of errors, as their true reflectivity can differ significantly from the calibration provided by the manufacturer. For example, the measured reflectivity of WS-1-LS is 2% lower at 380 nm and 5% lower at 300 nm than the values provided by the manufacturer. The manufacturer-provided reflectivity values for SRS-99 contained a small (<1%) dip between 260 and 290 nm that appears to be an artifact. Using these standards with their manufacturer-provided reflectivity values leads to >100% reflectivity for wavelengths below 300 nm (WS-1-LS), or a small peak between 260 and 290 nm (SRS-99). Both reflection standards were "certified reflection standards", although only the SRS-99 was

provided with a "reflection calibration certificate" (and calibrated against a NIST traceable standard within the last year). Other groups have measured decreased reflectivity in Spectralon samples over time [27], including samples that have not been exposed to high illumination levels. In fact, Spectralon samples stored in darkness have shown to degrade over time, and this is the most likely cause for the results presented in Fig. 13.

VI. Conclusions

We have measured the reflection coefficient for several commonly used reflectors. The reflectors were also screened for fluorescence and changing angular distribution with wavelength. The highest reflectivity for short wavelengths (<400 nm) was measured for the PTFE based reflectors, with the GORE® diffuse reflector having the highest reflectivity over the greatest wavelength range. PTFE based reflectors were the only examined reflectors that had >90% reflectivity for wavelengths below 300 nm, but all PTFE films exhibited decreasing reflectivity with increasing wavelength due to increased transmission for longer wavelengths. To achieve >95% reflectivity, the PTFE films have to be at least 0.5 mm thick. If a thinner diffuse reflector is needed, nitrocellulose is a good alternative.

Several of the reflectors have sharp declines in reflectivity below a cut-off wavelength, including TiO_2 (420 nm), ESR film (395 nm), nitrocellulose (330 nm), Lumirror® (325 nm), and Melinex® (325 nm). Lumirror®, Melinex®, and ESR film exhibited strong fluorescence, and Lumirror® and Melinex® also exhibited changing angular distributions with wavelength.

Acknowledgment

The mechanical construction of the setups presented in this paper was done by David Wilson. Dr. Jacob C. Jonsson, Johan Borglin, and Ilya Zorikhin-Nilsson assisted in the fluorescence and reflection measurements. Dr. William W. Moses contributed with invaluable discussions and suggestions.

This work was supported by the Director, Office of Science, Office of Biological and Environmental Research, Biological Systems Science Division of the U.S. Department of Energy under Contract No. DE-AC02-05CH11231.

References

[1] M. J. Weber and R. R. Monchamp. "Luminescence of Bi4Ge3O12 - Spectral and Decay Properties," Journal of Applied Physics, 44:5495-5499, 1973

[2] C. L. Melcher, J. S. Schweitzer, C. A. Peterson, R. A. Manente and H. Suzuki. Crystal growth and scintillation properties of the rare earth orthosilicates. Inorganic Scintillators and Their Applications, Delft Unviersity Press (SCINT95), ISBN 90-407-1215-8, :309-315, 1996.

[3] E. V. D. van Loef, P. Dorenbos, C. W. E. van Eijk, K. W. Kramer and H. U. Gudel. "Scintillation properties of LaBr3 : Ce3+ crystals: fast, efficient and high-energy-resolution scintillators," Nuclear Instruments & Methods in Physics Research Section A-Accelerators Spectrometers Detectors and Associated Equipment, 486:254-258, 2002.

[4] J. T. M. d. Haas and P. Dorenbos. Advances in Yield Calibration of Scintillators. IEEE Trans Nucl Sci, 55:1086-1092, 2008.

[5] C. L. Melcher and J. S. Schweitzer. Cerium-Doped Lutetium Oxyorthosilicate - a Fast, Efficient New Scintillator. IEEE Transactions on Nuclear Science, 39:502-505, 1992.

[6] B. C. Grabmaier. Crystal Scintillators. IEEE Transactions on Nuclear Science, 31:372-376, 1984.

[7] M. Janecek and W.W. Moses, "Optical Reflectance Measurements for Commonly Used Reflectors," IEEE Trans. Nucl. Sci, vol. 55, no. 4, pp. 2432-2437, Aug. 2008

[8] W. Budde, "Standards of reflectance," J. Opt. Soc. Am. **50**, 217-(1960)

[9] J. B. Gillespie, J. D. Lindberg, and L. S. Laude, "Kubelka-Munk Optical Coefficients for a Barium Sulfate White Reflectance Standard," Appl. Opt. **14**, 807-809 (1975)

[10] E. M. Patterson, C. E. Shelden, and B. H. Stockton, "Kubelka-Munk optical properties of a barium sulfate white reflectance standard," Appl. Opt. **16**, 729-732 (1977)

[11] F. Grum and G. W. Luckey, "Optical Sphere Paint and a Working Standard of Reflectance," Appl. Opt. **7**, 2289-2294 (1968)

[12] W. Erb, "Requirements for Reflectance Standards and the Measurement of Their Reflection Values," Applied Optics, 14 (2). 1975

[13] Bureau Central de la Commission Internationale de l'Eclairage, *Review of Publications on Properties and Reflection Values of Material Reflection Standards* (Paris, 1979), CIE Publication 46 (TC-2.3), pp. 15-72.

[14] J. B. Schutt, J. F. Arens, C. M. Shai, and E. Stromberg, "Highly Reflecting Stable White Paint for the Detection of Ultraviolet and Visible Radiations," Appl. Opt. **13**, 2218-2221 (1974)

[15] F. Benford, G. P. Lloyd, and S. Schwarz, "Coefficients of Reflection of Magnesium Oxide and Magnesium Carbonate," J. Opt. Soc. Am. **38**, 445-445 (1948)

[16] F. Vratny and J. J. Kokalas, "The Reflectance Spectra of Metallic Oxides in the 300 to 1000 Millimicron Region," Appl. Spectrosc. **16**, 176-184 (1962)

[17] A. Zecchina, M. G. Lofthouse and F. S. Stone, "Reflectance spectra of surface states in magnesium oxide and calcium oxide," J. Chem. Soc., Faraday Trans. 1, 1975, 71, 1476-1490, DOI: 10.1039/F19757101476

[18] V.R. Weidner and J.J. Hsia, JJ, "Reflection Properties of Pressed Polytetrafluoroethylene Powder," J. Opt. Soc. Amer., vol. 71, no. 7, pp. 856-861, 1981

[19] B. Waldwick, C. Chase, and B. Chang, "Increased efficiency and performance in laser pump chambers through use of diffuse highly reflective materials," in Proc. SPIE, 2007, vol. 6663, pp. 66630N.1–66630N.7.

[20] "A Guide to Reflectance Coatings and Materials," Labsphere, Reflections Newsletter, pp. 8-11, Sep. 1998

[21] A. L. Companion, and R. E. Wyatt, "The diffuse reflectance spectra of some titanium oxides," J. Phys. Chem. Solids, 24 (8), pp. 1025-1028, 1963

[22] J. Tickner, and G. Roach, "PHOTON An optical Monte Carlo code for simulating scintillation detector responses," Nucl. Instr. and Meth. in Phys. Res. B, 263, pp149-155, 2007

[23] A. Chavarria, "A study on the reflective properties of Tyvek in air and underwater", Dissertation, Duke University, 2007

[24] M. F. Weber, C. A. Stover, L. R. Gilbert, T. J. Nevitt, and A. J. Ouderkirk, "Giant Birefringent Optics in Multilayer Polymer Mirrors," Science, 287 (5462), pp. 2451-2456, 2000

[25] D. Motta, C. Buck, F.X. Hartmann, Th. Lasserre, S. Schonert, U. Schwan, "Prototype scintillator cell for an In-based solar neutrino detector," Nucl Instr Meth Phys Res A, 547 (2-3), Aug 2005, pp 368-388, ISSN 0168-9002, DOI: 10.1016/j.nima.2005.03.166.

[26] D.H. Goldstein, D.B. Chenault and J.L. Pezzaniti, "Polarimetric characterization of Spectralon," Proc. SPIE 3754, 126 (1999); doi:10.1117/12.366323

[27] W. Möller, K.-P. Nikolaus, and A. Höpe, "Degradation of the diffuse reflectance of Spectralon under low-level irradiation," Metrologia, 40, pp. 212-215, Feb. 2003

DISCLAIMER